

Geometric Visualization of a Robot End-Effector Motion using the Curvature Theory

Taha M. El-Adawy* and A. Shehata

**Department of Mathematics, College of Science and Arts in Unaizah, Qassim University,
Qassim, Kingdom of Saudi Arabia.*

Abstract. This investigation is devoted to the construction of a robot trajectory using a ruled surface. Transition relations among surface trihedron, tool trihedron, generator trihedron, natural trihedron and also Darboux vectors for each trihedron are given. Then, the curvature theory of ruled surface under investigation is applied to determine the differential properties of a robot end effector motion. This information is then used to characterize the linear motion of the tool center point and the angular motion of the tool frame of the robot end effector for the trajectory planning. The differential motion properties of the tool frame and the TCP point, based on the curvature theory of a ruled surface, using the relationships between the four frames of reference are studied.

AMC: 53A05, 53A17, 53B30

Keywords: Ruled surface, Darboux vector and curvatures, Robot trajectory planning, Robot end-effector.

1. Introduction

Here, we present the relation between ruled surface and robot trajectory [5-8].

The motion of robot end-effector is referred to as the robot trajectory. A robot trajectory consists of:

(i) A sequence of positions, velocities, accelerations of a fixed point in the end-effector.

(ii) A sequence of orientations, angular velocities and accelerations of the end-effector.

The fixed point in the end-effector will be referred to as the tool center point and is denoted by TCP. The orientation of the end-effector is best described by a coordinate frame attached to the end-effector, referred to as the tool frame.

The location and orientation of the robot end-effector are completely described using the tool frame and the tool center point (TCP). The tool frame consists of three unit vectors; namely, the orientation vector \underline{O} , the approach vector \underline{A} and the normal vector \underline{N} . The tool center point is chosen to be the origin of the tool frame.

The robot trajectory may be represented using a ruled surface. Each of the three unit vectors of the tool frame generates a ruled surface while the three ruled surfaces share a common directrix traced (trajectory) by the TCP. It is not necessary to use all three ruled surfaces to represent a robot trajectory; in fact, one ruled surface will suffice. As shown in Figure 2, the ruled surface generated by the approach vector \underline{A} is chosen here to represent the trajectory. We may note, however, that the orientation of other vectors, \underline{O} and \underline{N} , are not specified yet. Theoretically, this is because a robot end-effector motion, in general, has six degrees of freedom in space while a ruled surface provides only five independent parameters. Therefore, a robot trajectory may be completely described by adding one parameter to specify the orientation of the two vectors. The additional parameter is referred to, in this study, as the spin angle and is denoted by η . The spin angle is measured from the surface normal vector \underline{S}_n of the ruled surface to the normal vector \underline{N} . The ruled surface and the spin angle, which completely describes a robot trajectory, respectively, are

$$\underline{X}(s, v) = \underline{\alpha}(s) + v\underline{R}(s), \eta = \eta(s) \quad (1.1)$$

where $\underline{\alpha}$ is the directrix, v is a real-value parameter, and \underline{R} is the ruling (see figure 1) [1-4].

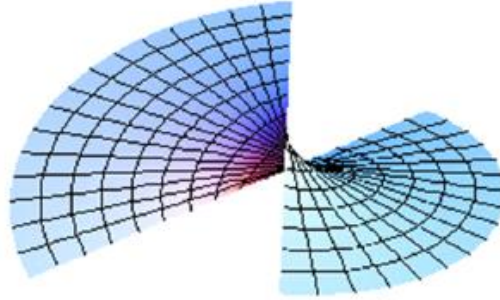


Figure (1). The ruled surface X

We choose the approach vector \underline{A} , to be the ruling. Any one of the three vectors in the tool frame could be chosen as the ruling and the spin angle describes the orientation of the other two vectors in cyclic order.

Each vector of tool frame in the end-effector defines its own ruled surface while robot moves. The path of tool center point is the directrix and \underline{A} is the ruling. As $\underline{\alpha}(s)$ is a curve and $\underline{R}(s)$ is straight line, let us consider the ruled surface (1.1).

The normalized parameter s may be based on the directrix $\underline{\alpha}$ or on the ruling \underline{R} as in the following respectively

$$s(\varphi) = \int_0^{\varphi} \left| \frac{d\underline{\alpha}(\varphi)}{d\varphi} \right| d\varphi, \quad (1.2)$$

$$s(\varphi) = \int_0^{\varphi} \left| \frac{d\underline{R}(\varphi)}{d\varphi} \right| d\varphi. \quad (1.3)$$

Through out this paper we use the normalized parameter as in (1.3) [16-19].

2. Reference Frames

In what follows, we construct the differential formulas of the following frames:

- (i) The tool frame $(\underline{Q}, \underline{A}, \underline{N})$

- (ii) The surface frame $(\underline{A}, \underline{S}_n, \underline{S}_b)$
- (iii) The generator trihedron $(\underline{r}, \underline{t}^*, \underline{t}_c)$
- (iv) The natural trihedron $(\underline{t}^*, \underline{n}^*, \underline{b}^*)$.

These frames are essential in the study of the motion of the end-effector.

Therefore we present the construction of these frames in a brief account [9-14].

2.1 Surface frame

To determine the orientation of the tool frame relative to the ruled surface $X = X(v, s)$, we define a surface frame at the TCP as shown in Figure 2.

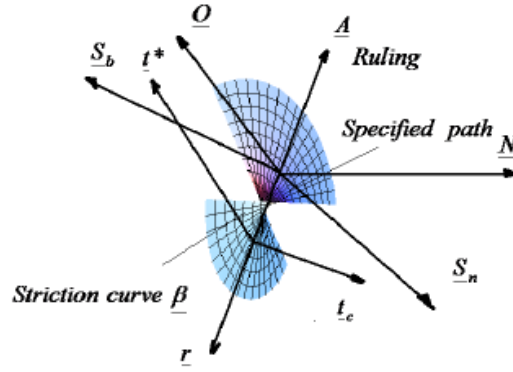


Figure 2. The orientation of the robot end-effector through the surface X.

The surface frame is defined by three orthogonal unit vectors, the approach vector \underline{A} , the surface normal vector \underline{S}_n , and their binormal vector \underline{S}_b . The surface normal vector is determined using the definition of the normal vector field to the ruled surface X as the following

$$\underline{S}_n = \frac{\underline{X}_v \wedge \underline{X}_s}{|\underline{X}_v \wedge \underline{X}_s|} \quad (2.1)$$

Thus, the surface binormal vector is given as

$$\underline{S}_b = \underline{S}_n \wedge \underline{A} \quad (2.2)$$

where $\underline{X}_v = \frac{\partial X}{\partial v}$, $\underline{X}_s = \frac{\partial X}{\partial s}$.

2.2 Frenet frame

The Frenet frame along the directrix $\underline{\alpha}$ is defined by three orthogonal unit vectors, namely; the tangent vector \underline{t} , the normal vector \underline{n} and the binormal vector \underline{b} as the following

$$\underline{t} = \underline{\alpha}', \underline{n} = \frac{\underline{t}'}{k}, \underline{b} = \underline{t} \wedge \underline{n}, ' = \frac{d}{ds} \quad (2.3)$$

where $k = |\underline{t}'|$ is the curvature of the directrix $\underline{\alpha} = \underline{\alpha}(s)$ (natural parametrization).

2.3 Generator trihedron

Generator trihedron moves along the striction curve and is used to study the positional and angular variation of ruled surface X . The generator trihedron is defined by three orthogonal unit vector, namely; the generator vector \underline{r} , the central normal vector \underline{t}^* and the central tangent vector \underline{k} . Since the ruling is not necessarily a unit vector, the generator vector is defined as

$$\underline{r} = \frac{\underline{R}}{|\underline{R}|} \quad (2.4)$$

Without loss of generality, we take \underline{R}' as a unit vector and the central normal vector \underline{t}^* is defined as

$$\underline{t}^* = \underline{R}' \quad (2.5)$$

The central tangent vector is given as

$$\underline{t}_c = \underline{r} \wedge \underline{t}^* \quad (2.6)$$

The striction curve $\underline{\beta} = \underline{\beta}(s)$ of the ruled surface (1.1) is defined as [2-4]

$$\underline{\beta}(s) = \underline{\alpha}(s) - \mu(s)\underline{R}(s) \quad (2.7)$$

where μ is a real valued parameter. The distance from the striction curve to the directrix α along the ruling is μR where $R = |\underline{R}| = \text{const}$. Thus, from the definition of the striction curve ($\langle \underline{\beta}', R' \rangle = 0$) we have

$$\mu = \langle \underline{\alpha}', R' \rangle / |R'|. \quad (2.8)$$

Differentiating Equation (2.7) gives first order positional variation of the striction point $\underline{\beta}'$ of the ruled surface (1.1) which can be expressed in the generator trihedron as in the following ,

$$\underline{\beta}' = \Gamma \underline{r} + \Delta \underline{t}_c \quad (2.9)$$

where

$$\Gamma = \frac{1}{R} \langle \underline{\alpha}', R \rangle - \mu' R, \Delta = \frac{1}{R} [\underline{\alpha}', R, R'] \quad (2.10)$$

From the motion of the generator trihedron and the striction curve one can obtain the differential motion of the end-effector in a simple and systematic manner. The first-order angular variation of the generator trihedron can be determined in the following matrix equation

$$\frac{d}{ds} \begin{pmatrix} \underline{r} \\ \underline{t}^* \\ \underline{t}_c \end{pmatrix} = \frac{1}{R} \begin{pmatrix} 0 & 1 & 0 \\ -1 & 0 & \gamma \\ 0 & -\gamma & 0 \end{pmatrix} \begin{pmatrix} \underline{r} \\ \underline{t}^* \\ \underline{t}_c \end{pmatrix} = U_r \wedge \begin{pmatrix} \underline{r} \\ \underline{t}^* \\ \underline{t}_c \end{pmatrix} \quad (2.11)$$

where the invariant

$$\gamma = \langle R'', (R \wedge R') \rangle = [R'', R, R'] \quad (2.12)$$

is called the geodesic curvature of the ruled surface X .

Using the relation between the vector product and the product of matrices, one can obtain

$$U_r = \frac{\gamma}{R} \underline{r} + \frac{1}{R} \underline{t}_c \quad (2.13)$$

which is called the Darboux vector of (axis of rotation) the generator trihedron.

2.4 Darboux frame for the ruled surface X

The Darboux frame for a curve $X(s, v(s))$ on the ruled surface X is defined by three orthogonal unit vectors, namely; the tangent vector \underline{T} of the curve, the normal vector \underline{S}_N on the surface X and the geodesic vector \underline{n}_g such that

$$\underline{T} = \frac{dX}{ds} = \underline{t} + v\underline{t}^* + \frac{v'}{R}\underline{r}, \quad (2.14)$$

$$\underline{S}_N = \frac{X_v \wedge X_s}{|X_v \wedge X_s|} = \frac{1}{\Pi} ((\mu - v | R |) \underline{t}_c - \Delta \underline{t}^*), \quad (2.15)$$

$$\begin{aligned} \underline{n}_g = \underline{T} \wedge \underline{S}_N = & \frac{1}{\Pi} ((\mu - v | R |) (\underline{t} \wedge \underline{t}_c) - \Delta (\underline{t} \wedge \underline{t}^* + v(\mu - v | R |) \underline{r} + \\ & \frac{v'(\mu - v | R |)}{|R|} \underline{t}^* - \frac{v'\Delta}{|R|} \underline{t}_c)) \end{aligned} \quad (2.16)$$

where $\Pi = \sqrt{(\mu - v | R |)^2 + \Delta^2}$ and $v = v(s)$.

2.5 Central normal surface and the natural trihedron

The natural trihedron is used to study the angular and positional variation of the central normal surface. As the generator trihedron moves along the striction curve $\underline{\beta} = \underline{\beta}(s)$, the central normal vector generates another ruled surface called the central normal surface and is denoted by \underline{X}_T . The central normal surface, is defined as

$$\underline{X}_T(s, v) = \underline{\beta}(s) + v\underline{t}^*(s) \quad (2.17)$$

where $\underline{\beta} = \underline{\beta}(s)$ is the position vector of the striction curve of the original ruled surface X , and v is a real parameter (see figure 3).

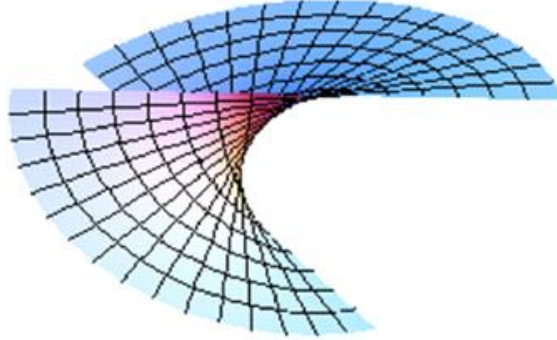


Figure (3). The central normal surface X_T

The location of the striction curve of the central normal surface \underline{X}_T relative to the striction curve $\underline{\beta} = \underline{\beta}(s)$ of the ruled surface X is given by

$$\underline{\beta}_T(s) = \underline{\beta}(s) - \mu_T \underline{t}^*(s) \quad (2.18)$$

where

$$\mu_T(s) = \left| \frac{\langle \underline{\beta}', \underline{t}^{*'} \rangle}{\langle \underline{t}^{*'}, \underline{t}^{*'} \rangle} \right|. \quad (2.19)$$

From equation (2.9) and (2.11) we have

$$\mu_T(s) = \frac{-R(\Gamma + \Delta\gamma)}{1 + \gamma^2}, \gamma \neq \pm i \quad (2.20)$$

The natural trihedron is defined by three orthogonal unit vectors, namely; the central normal vector \underline{t}^* , the principal normal vector \underline{n}^* and the binormal vector \underline{b}^* as shown in figure 4 such that

$$\underline{t}^* = \underline{R}', \underline{n}^* = \frac{1}{\kappa^*} \underline{t}^{*'}, \underline{b}^* = \underline{t}^* \wedge \underline{n}^* \quad (2.21)$$

where $\kappa^* = |\underline{t}'^*|$.

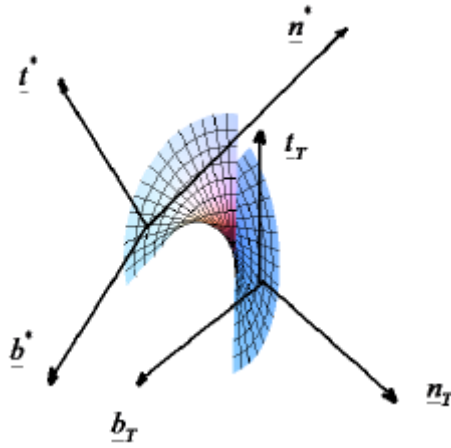


Figure (4). The central normal surface X_T and its reference: frames.

The Frenet frame for the curve $\beta = \beta(s)$ on the Central normal surface X_T is defined through the tangent vector \underline{t}_T , the normal vector \underline{n}_T and the binormal vector \underline{b}_T where

$$\begin{aligned} \underline{t}_T &= \underline{\beta}' = \underline{t} - \mu' |R| \underline{r} - \mu \underline{t}^*, \\ \underline{n}_T &= \frac{\underline{t}_T'}{k_T} = k \underline{n} + \left(\frac{\mu}{|R|} - \mu'' |R| \right) \underline{r} - 2\mu' \underline{t}^* - \frac{\mu \gamma}{|R|} \underline{t}_c, \quad k_T = |\underline{t}_T'|, \\ \underline{b}_T &= \underline{n}_T \wedge \underline{t}_T. \end{aligned} \quad (2.22)$$

2.6 Darboux frame for the central normal surface X_T

The Darboux frame for a curve $X_T(s, v(s))$ on the ruled surface X_T is defined by three orthogonal unit vectors, namely; the tangent vector \underline{T}_T , the normal vector \underline{S}_{NT} and the geodesic vector \underline{n}_{gT} such that

$$\begin{aligned}
\underline{T}_T &= \frac{dX_T}{ds} = \left(\Gamma - \frac{\nu}{|R|}\right)r - \nu \underline{t}^* + \left(\Delta + \frac{\gamma\nu}{|R|}\right)\underline{t}_c, \\
\underline{S}_{NT} &= \frac{1}{\prod_T} \left(\left(\frac{\nu}{|R|} - \Gamma\right)\underline{t}_c + \left(\Delta + \frac{\gamma\nu}{|R|}\right)r \right), \\
\underline{n}_g &= \underline{T}_T \wedge \underline{S}_{NT} \\
&= \frac{1}{\prod_T} \left[\prod_T^2 \underline{t}^* + \nu \left(\frac{\nu}{|R|} - \Gamma\right)r - \nu \left(\Delta + \frac{\gamma\nu}{|R|}\right)\underline{t}_c \right]
\end{aligned} \tag{2.23}$$

where $\prod_T = \sqrt{\left(\frac{\nu}{|R|} - \Gamma\right)^2 + \left(\Delta + \frac{\gamma\nu}{|R|}\right)^2}$.

Let the rotation angle ρ between the vectors \underline{r}^* and \underline{b}^* , thus we have

$$\begin{aligned}
\underline{r} &= \cos\rho \underline{b}^* - \sin\rho \underline{n}^* \\
\underline{t}_c &= \cos\rho \underline{n}^* + \sin\rho \underline{b}^*
\end{aligned} \tag{2.24}$$

Equation (2.24) can be written in the matrix form as

$$\begin{pmatrix} \underline{r} \\ \underline{t}_c^* \\ \underline{t}_c \end{pmatrix} = \begin{pmatrix} 0 & -\sin\rho & \cos\rho \\ 1 & 0 & 0 \\ 0 & \cos\rho & \sin\rho \end{pmatrix} \begin{pmatrix} \underline{t}_c^* \\ \underline{n}^* \\ \underline{b}^* \end{pmatrix} \tag{2.25}$$

The inverse of the linear transformation (2.25) is given as

$$\begin{pmatrix} \underline{t}_c^* \\ \underline{n}^* \\ \underline{b}^* \end{pmatrix} = \begin{pmatrix} 0 & 1 & 0 \\ -\sin\rho & 0 & \cos\rho \\ \cos\rho & 0 & \sin\rho \end{pmatrix} \begin{pmatrix} \underline{r} \\ \underline{t}_c^* \\ \underline{t}_c \end{pmatrix} \tag{2.26}$$

From equation (2.11) and (2.26) we obtain

$$\underline{t}_c^* \iota = \frac{1}{R} (-\underline{r} + \gamma \underline{t}_c) = \kappa^* \underline{n} = \kappa^* (-\sin\rho \underline{r} + \cos\rho \underline{t}_c). \tag{2.27}$$

From this equality we have

$$\sin\rho = \frac{1}{R\kappa^*}, \quad \cos\rho = \frac{\gamma}{R\kappa^*}. \quad (2.28)$$

Then the geodesic curvature of the ruled surface X can be written as

$$\gamma = \cot\rho. \quad (2.29)$$

From equation (2.28) and equation (2.13) we get

$$\frac{d}{ds} \begin{pmatrix} \underline{r} \\ \underline{t}^* \\ \underline{t}_c \end{pmatrix} = \frac{1}{R} \begin{pmatrix} 0 & 1 & 0 \\ -1 & 0 & \cot\rho \\ 0 & -\cot\rho & 0 \end{pmatrix} \begin{pmatrix} \underline{r} \\ \underline{t}^* \\ \underline{t}_c \end{pmatrix} = U_r \wedge \begin{pmatrix} \underline{r} \\ \underline{t}^* \\ \underline{t}_c \end{pmatrix} \quad (2.30)$$

From equation (2.22) we have

$$\mu_T(s) = -R\sin^2\rho(\Gamma + \Delta\cot\rho) \quad (2.31)$$

Also by equation (2.28), one can obtain the curvature k^* of the ruled surface X as in the following

$$\kappa^* = \frac{\sqrt{1+\gamma^2}}{R} = \frac{1}{R\sin\rho}. \quad (2.32)$$

The first-order angular variation of natural trihedron may be expressed in the matrix form as

$$\frac{d}{ds} \begin{pmatrix} \underline{t}^* \\ \underline{n}^* \\ \underline{b}^* \end{pmatrix} = \begin{pmatrix} 0 & \kappa^* & 0 \\ -\kappa^* & 0 & \tau^* \\ 0 & \tau^* & 0 \end{pmatrix} \begin{pmatrix} \underline{t}^* \\ \underline{n}^* \\ \underline{b}^* \end{pmatrix} = U_t \wedge \begin{pmatrix} \underline{t}^* \\ \underline{n}^* \\ \underline{b}^* \end{pmatrix} \quad (2.33)$$

where U_t is the Darboux vector of the natural trihedron and is given by

$$U_t = \tau^* \underline{t}^* + \kappa^* \underline{b}^*. \quad (2.34)$$

From equation (2.25) and (2.28) we have

$$\begin{pmatrix} \underline{r} \\ \underline{t}^* \\ \underline{t}_c \end{pmatrix} = \frac{1}{R\kappa^*} \begin{pmatrix} 0 & -1 & \gamma \\ R\kappa^* & 0 & 0 \\ 0 & \gamma & 1 \end{pmatrix} \begin{pmatrix} \underline{t}^* \\ \underline{n}^* \\ \underline{b}^* \end{pmatrix}. \quad (2.35)$$

From equation (2.20),(2.29) and (2.31) one can see that the first order positional variation of the striction curve β_T of central normal surface X_T is given as

$$\underline{\beta}'_T = \Gamma_T \underline{t}^* + \Delta_T \underline{b}^* \quad (2.36)$$

where

$$\Gamma_T = \mu'_T, \quad \Delta_T = \frac{\gamma\Gamma - \Delta}{\sqrt{1+\gamma^2}}. \quad (2.37)$$

The curvature k^* and the torsion τ^* of the ruled surface X are given respectively as

$$\kappa^{*2} = \frac{\langle (\underline{R}' \wedge \underline{R}''), (\underline{R}' \wedge \underline{R}'') \rangle}{(\langle \underline{R}', \underline{R}' \rangle)^3} \quad (2.38)$$

$$\tau^* = \frac{[\underline{R}''', \underline{R}', \underline{R}'']}{\langle (\underline{R}' \wedge \underline{R}''), (\underline{R}' \wedge \underline{R}'') \rangle}. \quad (2.39)$$

Observe that the Darboux vector U_r of the generator trihedron and the Darboux vector U_t of the natural trihedron, describe the angular motion of the ruled surface X and the central normal surface X_T , respectively. Therefor, the Darboux vector may be considered as the angular velocity where as the positional variation β_T' of the striction curve may be considered as the linear velocity.

The curvature k_T , geodesic curvature γ_T and the torsion τ_T of the central normal surface X_T are given respectively from

$$\kappa_T^2 = \frac{\langle (\underline{t}^* \wedge \underline{t}^{*'})', (\underline{t}^* \wedge \underline{t}^{*'}) \rangle}{(\underline{t}^* \wedge \underline{t}^{*'})^3}, \quad (2.40)$$

$$\gamma_T = \langle (\underline{t}^{*''}), (\underline{t}^* \wedge \underline{t}^{*'}) \rangle = [\underline{t}^{*''}, \underline{t}^*, \underline{t}^{*'}], \quad (2.41)$$

$$\tau_T = \frac{[\underline{t}^{*''}, \underline{t}^{*'}, \underline{t}^{*''}]}{\langle (\underline{t}^* \wedge \underline{t}^{*''}), (\underline{t}^* \wedge \underline{t}^{*''}) \rangle}. \quad (2.42)$$

Remark 2.1 The functions, Δ_T and Γ_T and κ^* and τ^* , play the same role as the curvature function of the central normal surface X_T .

3. Relationship between the Frames of Reference

Here, we give the orientation of the surface frame relative to the tool frame and the generator trihedron. For this purpose, let ϕ be the angle between the vectors \underline{S}_b and \underline{O} , i.e.,

$$\langle \underline{S}_b, \underline{O} \rangle = \cos \phi \quad (3.1)$$

which leads to the following

$$\begin{aligned} \underline{O} &= \cos \phi \underline{S}_n + \sin \phi \underline{S}_b \\ \underline{N} &= \underline{O} \wedge \underline{A} = -\sin \phi \underline{S}_n + \cos \phi \underline{S}_b. \end{aligned} \quad (3.2)$$

These relations can be summarized in the non singular linear transformation

$$\begin{pmatrix} \underline{A} \\ \underline{O} \\ \underline{N} \end{pmatrix} = \begin{pmatrix} 1 & 0 & 0 \\ 0 & \cos \phi & \sin \phi \\ 0 & -\sin \phi & \cos \phi \end{pmatrix} \begin{pmatrix} \underline{A} \\ \underline{S}_n \\ \underline{S}_b \end{pmatrix}. \quad (3.3)$$

Similarly, let ψ be the angle between the vectors \underline{S}_b and \underline{t}_c thus we have

$$\begin{pmatrix} \underline{A} \\ \underline{S}_n \\ \underline{S}_b \end{pmatrix} = \begin{pmatrix} 1 & 0 & 0 \\ 0 & \cos\psi & \sin\psi \\ 0 & -\sin\psi & \cos\psi \end{pmatrix} \begin{pmatrix} \underline{r} \\ \underline{t}^* \\ \underline{t}_c \end{pmatrix}. \quad (3.4)$$

From the equations (3.4) and (3.2) we get

$$\begin{pmatrix} \underline{A} \\ \underline{O} \\ \underline{N} \end{pmatrix} = \begin{pmatrix} 1 & 0 & 0 \\ 0 & \cos\theta & \sin\theta \\ 0 & -\sin\theta & \cos\theta \end{pmatrix} \begin{pmatrix} \underline{r} \\ \underline{t}^* \\ \underline{t}_c \end{pmatrix} \quad (3.5)$$

where $\theta = \phi + \psi$.

The inverse of this linear transformation is given as

$$\begin{pmatrix} \underline{r} \\ \underline{t}^* \\ \underline{t}_c \end{pmatrix} = \begin{pmatrix} 1 & 0 & 0 \\ 0 & \cos\theta & -\sin\theta \\ 0 & \sin\theta & \cos\theta \end{pmatrix} \begin{pmatrix} \underline{A} \\ \underline{O} \\ \underline{N} \end{pmatrix} \quad (3.6)$$

where θ , referred as spin angle, describes the orientation of the end-effector.

Substituting the partial derivatives of Equation (2.1) into (2.4) we have

$$\underline{S}_n = \frac{\mu \underline{t}_c - \Delta \underline{t}^*}{\sqrt{\mu^2 + \Delta^2}}, \quad \underline{S}_b = \underline{S}_n \wedge \underline{O} = \frac{\mu \underline{t}^* - \Delta \underline{t}_c}{\sqrt{\mu^2 + \Delta^2}}. \quad (3.7)$$

From the equations (3.4),(3.7) and (3.8) we get

$$\cos\psi = \frac{-\Delta}{\sqrt{\mu^2 + \Delta^2}}, \quad \sin\psi = \frac{\mu}{\sqrt{\mu^2 + \Delta^2}}, \quad \psi = \tan^{-1}\left(\frac{-\mu}{\Delta}\right). \quad (3.8)$$

4. Differential Properties of the Robot End Effector Motion [15-20]

The motion of the robot end effector is described by the angular motion of the tool frame and the linear motion of the TCP. In this section, the differential motion properties of the tool frame and TCP of first and second order, i.e., $\underline{\alpha}'$ and $\underline{\alpha}''$ are studied.

Since the directrix $\underline{\alpha}$ is the locus of the TCP and from equation (2.9) we obtain

$$\underline{\alpha}'(s) = \underline{\beta}' + \underline{\mu}'R + \underline{\mu}t. \quad (4.1)$$

Using Eq(2.10) we get

$$\underline{\alpha}'(s) = (\Gamma + \underline{\mu}'R)\underline{r} + \underline{\mu}t^* + \Delta t_c. \quad (4.2)$$

From Eq(3.6) we have

$$\underline{\alpha}'(s) = (\Gamma + \underline{\mu}'R)\underline{A} + (\underline{\mu}\cos\theta + \Delta\sin\theta)\underline{O} - (\underline{\mu}\sin\theta - \Delta\cos\theta)\underline{N} \quad (4.3)$$

The first order angular variation of the tool frame is determined from Eq(3.5) as in the following

$$\frac{d}{ds} \begin{pmatrix} \underline{A} \\ \underline{O} \\ \underline{N} \end{pmatrix} = \frac{1}{R} \begin{pmatrix} 0 & 1 & 0 \\ 0 & -\Omega R \sin\theta & \Omega R \cos\theta \\ \sin\theta & -\Omega R \cos\theta & \Omega R \sin\theta \end{pmatrix} \begin{pmatrix} \underline{r} \\ \underline{t}^* \\ \underline{t}_c \end{pmatrix} \quad (4.4)$$

where $\Omega = \theta' + \frac{\gamma}{R}$. From Eq(3.6) we have

$$\frac{d}{ds} \begin{pmatrix} \underline{A} \\ \underline{O} \\ \underline{N} \end{pmatrix} = \frac{1}{R} \begin{pmatrix} 0 & \cos\theta & -\sin\theta \\ -\cos\theta & 0 & \Omega R \\ \sin\theta & \Omega R & 0 \end{pmatrix} \begin{pmatrix} \underline{A} \\ \underline{O} \\ \underline{N} \end{pmatrix}. \quad (4.5)$$

The 1st order angular variation of the tool frame (4.5) can be written as

$$\frac{d}{ds} \begin{pmatrix} \underline{A} \\ \underline{O} \\ \underline{N} \end{pmatrix} = \underline{U}_o \wedge \begin{pmatrix} \underline{A} \\ \underline{O} \\ \underline{N} \end{pmatrix} \quad (4.6)$$

where

$$\underline{U}_o = \Omega \underline{A} + \frac{1}{R} (\sin \theta \underline{O} + \cos \theta \underline{N}) \quad (4.7)$$

is referred to as the Darboux vector of the tool frame.

From Eq(3.5) we get

$$\underline{U}_o = \Omega \underline{r} + \frac{1}{R} t_c. \quad (4.8)$$

Differentiate Eq(4.2) we get

$$\underline{\alpha}''(s) = (\Gamma' + \mu''R - \frac{\mu}{R}) \underline{r} + (\frac{\Gamma}{R} + 2\mu' + \frac{\Delta\gamma}{R}) \underline{t}_c^* + (\Delta' + \frac{\mu\gamma}{R}) \underline{t}_c. \quad (4.9)$$

From Eq(3.6), the 2nd derivative $\underline{\alpha}''$ can be expressed interms of the tool frame as the following

$$\underline{\alpha}''(s) = (\Gamma' + \mu''R - \frac{\mu}{R}) \underline{A} + [(\Delta' + \frac{\mu\gamma}{R}) \sin \theta - (\frac{\Gamma}{R} + 2\mu' + \frac{\Delta\gamma}{R}) \cos \theta] \underline{O} + \underline{N}. \quad (4.10)$$

From Eq(4.8) we obtain

$$\underline{U}_o' = \Omega' \underline{r} + \frac{\theta'}{R} t_c. \quad (4.11)$$

It is well-known that the robot trajectory planning is based on time-dependent properties, e.g., velocity, acceleration, angular velocity, and angular acceleration, of robot end effector motion. Therefore the time-dependent motion properties of the end effector can be determined by applying the chain rule to the differential motion properties determined in (4.2).

The velocity \underline{V} and acceleration \underline{a} of TCP, and angular velocity \underline{w} and acceleration \underline{g} of the end effector are determined, respectively as

$$\underline{V} = \underline{\alpha}' \dot{s} = \dot{s}((\Gamma + \mu'R) \underline{A} + (\mu \cos \theta + \Delta \sin \theta) \underline{O} - (\mu \sin \theta - \Delta \cos \theta) \underline{N}), \quad (4.12)$$

$$\begin{aligned}
\underline{a} &= \underline{\alpha}' \ddot{s} + \underline{\alpha}'' \dot{s}^2 = [\ddot{s}(\Gamma + \mu'R) + \dot{s}^2(\Gamma' + \mu''R - \frac{\mu}{R})]\underline{A} \\
&+ [\ddot{s}(\mu \cos \theta + \Delta \sin \theta) + \dot{s}^2[(\Delta' + \frac{\mu\gamma}{R}) \sin \theta - (\frac{\Gamma}{R} + 2\mu' + \frac{\Delta\gamma}{R}) \cos \theta]]\underline{Q} \\
&+ [\ddot{s}(\Delta \cos \theta - \mu \sin \theta) + \dot{s}^2[(\frac{\Gamma}{R} + 2\mu' + \frac{\Delta\gamma}{R}) \sin \theta - (\Delta' + \frac{\mu\gamma}{R}) \cos \theta]]\underline{N} \quad (4.13)
\end{aligned}$$

$$\underline{w} = \underline{U}_o \dot{s} = \dot{s}(\underline{\Omega}r + \frac{1}{R}t_c), \quad (4.14)$$

$$\underline{g} = \underline{w} = \underline{U}_o \ddot{s} + \underline{U}_o' \dot{s}^2 = (\ddot{s}\Omega + \dot{s}^2\Omega')r + (\frac{1}{R}\ddot{s} + \dot{s}^2\frac{\theta'}{R})t_c \quad (4.15)$$

where $\dot{} = \frac{d}{dt}$ (differentiation with respect to time).

5. Application

Consider the ruled surface

$$\underline{X}(s, v) = \underline{\alpha}(s) + v\underline{R}(s) \quad (5.1)$$

where the directrix α coincides with the striction curve β and α is

$$\underline{\alpha}(s) = (\frac{-1}{\sqrt{2}} \sin \frac{s}{\sqrt{2}}, \frac{1}{\sqrt{2}} \cos \frac{s}{\sqrt{2}}, \frac{s}{\sqrt{2}}) \quad \text{and the generator } R \text{ is}$$

$$\underline{R}(s) = (\cos \frac{s}{\sqrt{2}}, \sin \frac{s}{\sqrt{2}}, 0) \quad \text{with } \langle \underline{R}, \underline{R} \rangle = 1. \quad \text{The generator trihedron}$$

(r, t^*, t_c) is given as the following

$$\begin{aligned}
\underline{r} &= (\cos \frac{s}{\sqrt{2}}, \sin \frac{s}{\sqrt{2}}, 0) \\
\underline{t}^* = \underline{R}' &= (\frac{-1}{\sqrt{2}} \sin \frac{s}{\sqrt{2}}, \frac{1}{\sqrt{2}} \cos \frac{s}{\sqrt{2}}, 0) \\
\underline{t}_c &= (0, 0, \frac{1}{\sqrt{2}}), \quad \text{constant vector} \quad (5.2)
\end{aligned}$$

From Eq(2.9), (2.11), (2.13), (2.39) and (2.40) it is easy to see the invariants of the end-effectors are given as the following

$$\begin{aligned}\Gamma &= \frac{-1}{2}, \Delta = \frac{1}{2} \\ \gamma &= 0, \mu = 0 \\ \kappa^* &= 1, \tau^* = 0, \mu_T = 1 \\ k_T &= 2, \tau_T = 0, \gamma_T = 0, \Delta_T = \frac{-1}{2}, \Gamma_T = 0.\end{aligned}\quad (5.3)$$

Remark 5.1 *The invariants of the robot end effectors under consideration are constants.*

The natural trihedron is given in the following form

$$\begin{aligned}\underline{t}^* &= \left(\frac{-1}{\sqrt{2}} \sin \frac{s}{\sqrt{2}}, \frac{1}{\sqrt{2}} \cos \frac{s}{\sqrt{2}}, 0 \right) \\ \underline{n}^* &= \left(\frac{-1}{2} \cos \frac{s}{\sqrt{2}}, \frac{-1}{2} \sin \frac{s}{\sqrt{2}}, 0 \right) . \\ \underline{b}^* &= \left(0, 0, \frac{1}{2\sqrt{2}} \right), \text{ constant vector}\end{aligned}\quad (5.4)$$

The central normal surface \underline{X}_T is given as

$$\underline{X}_T(s, v) = \underline{\beta} + v \underline{t}^* = \left(\frac{-1}{\sqrt{2}} \sin \frac{s}{\sqrt{2}}, \frac{1}{\sqrt{2}} \cos \frac{s}{\sqrt{2}}, \frac{s}{\sqrt{2}} \right) + v \left(\frac{-1}{\sqrt{2}} \sin \frac{s}{\sqrt{2}}, \frac{1}{\sqrt{2}} \cos \frac{s}{\sqrt{2}}, 0 \right) \quad (5.5)$$

From the definition of the striction curve $\beta_T(s)$ of the central normal surface $X_T(s)$ it is easy to see that $\beta_T(s) = \left(0, 0, \frac{s}{\sqrt{2}} \right)$ is a straight line in the directrix of \underline{b}^* and \underline{t}_c .

The Darboux vector of the generator trihedron is

$$\underline{U}_r = \left(0, 0, \frac{-1}{\sqrt{2}} \right), \text{ constant vector} \quad (5.6)$$

The Darboux vector of natural trihedron is

$$\underline{U}_t = \left(0, 0, \frac{-1}{2\sqrt{2}} \right), \text{ constant vector} \quad (5.7)$$

From Eq(3.19) and (5.3) we have $\tan \psi = 0$, *i.e.* $\psi = 0$ and $\psi' = 0$.

Since the spin angle ϕ between the tool frame and the surface normal zero, *i.e.*, $\phi = 0 \rightarrow \phi' = 0, \theta = \psi, \theta' = \psi', \Sigma' = 0$, then

$$\underline{O} = \left(\frac{-1}{\sqrt{2}} \sin \frac{s}{\sqrt{2}}, \frac{-1}{\sqrt{2}} \cos \frac{s}{\sqrt{2}}, 0 \right) \quad (5.8)$$

$$\underline{N} = \left(0, 0, \frac{1}{\sqrt{2}} \right), \text{ constant vector} \quad (5.9)$$

$$\begin{aligned} \underline{S}_n &= \left(\frac{1}{\sqrt{2}} \sin \frac{s}{\sqrt{2}}, \frac{-1}{\sqrt{2}} \cos \frac{s}{\sqrt{2}}, 0 \right) \\ \underline{S}_b &= \left(0, 0, \frac{-1}{\sqrt{2}} \right), \text{ constant vector} \end{aligned} \quad (5.10)$$

The first and second order positional variation of the TCP can be expressed in the tool frame as

$$\underline{\alpha}' = -\frac{1}{2} \underline{A} - \frac{1}{2} \underline{N} \quad (5.11)$$

$$\underline{\alpha}'' = \frac{1}{2} \underline{O} \quad (5.12)$$

The Darboux vector \underline{U}_o of the tool frame is a constant vector given as

$$\underline{U}_o = -\underline{N} = \underline{U}, \text{ and } \underline{U}'_o = 0 \quad (5.13)$$

The linear velocity and acceleration are given as

$$\begin{aligned} \underline{V} &= -\frac{\dot{s}}{2} \underline{A} - \frac{\dot{s}}{2} \underline{N}, \\ \underline{a} &= -\frac{\ddot{s}}{2} \underline{A} - \frac{\ddot{s}}{2} \underline{N} + \frac{\dot{s}^2}{2} \underline{O} \end{aligned} \quad (5.14)$$

The angular velocity \underline{w} and acceleration \underline{g} of the end effector are given by

$$\begin{aligned}\underline{w} &= -\dot{s}\underline{N}, \\ \underline{g} &= -\ddot{s}\underline{N}\end{aligned}\tag{5.15}$$

emark 5.2 *The Darboux vectors of the three frames attached to the robot end effector are constants and parallel to \underline{N} .*

Conclusion

From the curvature theory of ruled surface, one can see that the motion of the robot end-effector can be represented by the union of ruled surface X and its associated central normal surface X_T (figure 5). The configuration space consists of $X \cup X_T$ and the different frames with the orientation of the motion through the Darboux frames especially U_0 . The frame on configuration space is given in figure 6. The analytical representation is given through the frames $(\underline{r}, \underline{t}^*, \underline{t}_c)$, $(\underline{t}^*, \underline{n}^*, \underline{b}^*)$, $(\underline{A}, \underline{O}, \underline{N})$, $(\underline{U}_r, \underline{U}_t, \underline{U}_0)$ and the spin angle attached to the ruled surfaces X and X_T . From (5.15) it follows that the angular motion parallel to the constant Darboux vector $\underline{U}_0 = \underline{N}$.

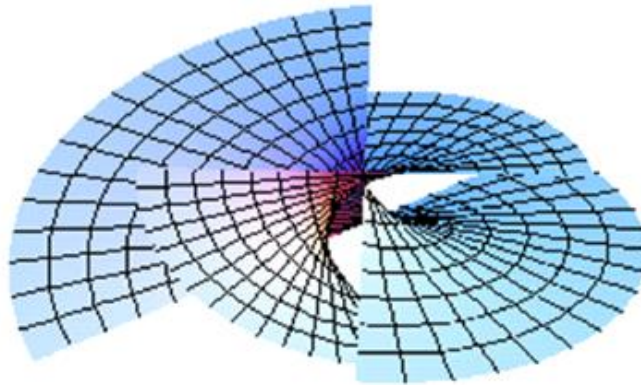


Figure (5). The configuration space $X \cup X_T$ of the robot end effector motion.

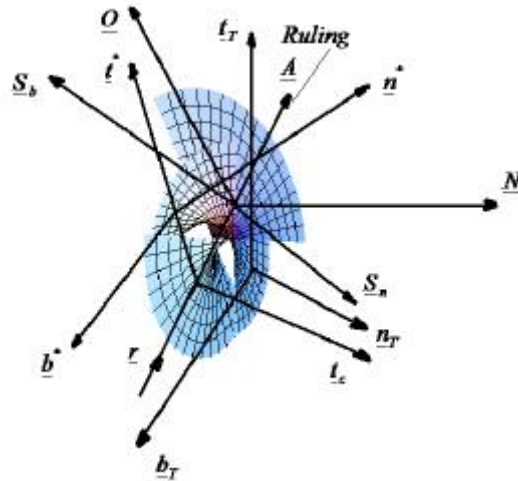


Figure (6). The different frames in the configuration space $X \cup X_T$ of the motion.

Acknowledgement

The Authors express their sincere appreciation to Prof. Dr. Nassar H. Abdel-All (Department of Mathematics, Faculty of Science, Assiut University, Assiut 71516, Egypt) for their kind interests, encouragements, helps, suggestions, comments and the investigations for this series of projects.

References

- [1] O.Kose, Contributions to the theory of integral invariants of a closed ruled surface, *Mechanism and Machine theory*, vol. 32, no. 2, pp.261-277, 1997.
- [2] F. L. Litvin and X. C. Gao, Analytical representation of trajectory of manipulators, trends and developments in mechanisms machines, and robotics in the ASME Design Technology Conferences, the 20th Biennial Mechanisms Conference, vol. 15-3, pp. 481-485, Kissimmee, Fla, USA, September 1988.
- [3] J. M. McCarthy, On the scalar and dual formulations of curvature theory of line trajectories, *Journal of Mechanisms, Transmissions, and Automation in Design*, vol.109, no. 1, pp.101-106, 1987.
- [4] M. McCarthy and B. Roth, The curvature theory of line Trajectories in spatial kinematics, *Journal of Mechanical Design*, vol. 103, no. 4, pp. 718-624, 1081.
- [5] Nassar H. Abdel-All, Rashed A. Abdel-Baky and F. M. Hamdoon, Ruled surfaces with timelike rullings. *Applied Math. and computations*, 147, 241-253, (2004).
- [6] Nassar H. Abdel-All, et. al, Dual construction of Developable Ruled surface,

Journal of American science 7(4), 789-793 (2011).

- [7] Nassar H. Abdel-All and F. M. Hamdoon, Cyclic surfaces in E5 generated by equiform motions. *Journal of geometry* Vol.79, 1-11, (2004).
- [8] Nassar H. Abdel-All and Fatma Mefrah, The geometry of Equiform motion, *Far East J. of Math. Science*, Vol.2, 431-438, May (2008).
- [9] Nassar H. Abdel-All and Haya R. Al-tameme, Line Intrinsic geometry of neighbouring surfaces, *Far East J. of Math Sciences* (November) Vol.31, No.2, 339-351(2008).
- [10] Nassar H. Abdel-All and Fatma Mefrah, Geometry of Helical motions. *Far East J of math* (December), Vol.31, No.3, 491-500 (2008).
- [11] Nassar H. Abdel-All and Haya R. Al-tameme, Geometry of incident line congruence, *Far East J. of math*, Vol.33, No.1, pp.41-54 (2009).
- [12] Nassar H. Abdel-All, Linear variations on an equiform motion, *Far East J of math* (September), Vol.34, No.3, 385-392 (2009).
- [13] Nassar H. Abdel-All, et al, Intersection curves of implicit and parametric surface in R3, *Applied Mathematics*, Vol.2, No.8, pp.1019-1026 (2011).
- [14] Nassar H. Abdel-All and Areej A. Al-moneef, Local study of singularities on an equiform motion. *Studies in Mathematical Sciences*, Vol. 5, No. 2, pp. 26-36 (2012).
- [15] R. Paul. "Manipulator Cartesian path control. *IEEE Transactions on System, Man and Cybernetics*, vol.9. no 11, pp.702-711, 1979.
- [16] B. S. Ryuh and G. R. Pennock, Accurate motion of a robot end- effector using the curvature theory of ruled surfaces" *Journal of Mechanisms, Transmission , and Automation in Design*, vol. 110, no. 4, pp.383-388, 1988.
- [17] B. S. Ryuh, Robot trajectory planning using the Curvature theory of ruled surfaces, Doctoral dissertation purdue University, West Lafayette, Ind, USA, 1989.
- [18] J. A. Schaaf, Curvature theory of line trajectories spatial kinematics, Doctoral dissertation, University of California, Davis, Calif, USA, 1988.
- [19] J. A. Schaaf and B. Rarani, Geometric Continuity of ruled surfaces, *Computer Aided Geometric Design*, vol.15, no. 3 , pp.289-310.
- [20] Vladimir M. Zatsiorsky; Kinematics of Human motion, Library of Congress (1998).

رؤية هندسية لحركة النهايات الطرفية للإنسان الآلي باستخدام نظرية الإنحناءات

طه العدوي - أيمن شحاتة

قسم الرياضيات-كلية العلوم والآداب بعنيزة - أقسام الطلاب- جامعة القصيم-المملكة العربية السعودية

ملخص البحث. البحث يهدف إلى بناء مسار لحركة الإنسان الآلي باستخدام سطح مسطر. وباستخدام مفاهيم الهندسة أمكن وصف الحركة من خلال العلاقات المتبادلة بين الإطارات المتحركة وكذلك وصف الدوران من خلال متجه داربو لكل إطار. وباستخدام هذه المعلومات أمكن الحصول على الحركة الخطية والحركة الزاوية متمثلة في السرعة والتسارع الخطي والزاوي. الإطارات الأربعة وفراغ الحركة أمكن الحصول عليها ورسمها باستخدام البرامج المساعدة في الهندسة والحاسب.

